Annals of Nuclear Energy 174 (2022) 109157

Contents lists available at ScienceDirect

Annals of Nuclear Energy

journal homepage: www.elsevier.com/locate/anucene

Uncertainty analyses of neutron noise simulations in a Zero-Power reactor

S. Yum [a], M. Hursin [b], A. Vasiliev [b], P. Vinai [c], A.G. Mylonakis [c], C. Demazière [c,*], R. Macián-Juan [a]

[a] Technical University of Munich, Garching, Germany
[b] Paul Scherrer Institute, Villigen, Switzerland
[c] Chalmers University of Technology, Gothenburg, Sweden

ARTICLE INFO

Article history:
Received 18 January 2022
Received in revised form 1 April 2022
Accepted 18 April 2022
Available online 10 May 2022

Keywords:
Uncertainty analyses
Fuel rods vibration
Uncertainty propagation
Sensitivity analyses
Neutron noise
Neutron flux oscillation

ABSTRACT

A comprehensive uncertainty analysis methodology has been established for the modeling of stationary neutron flux oscillations induced by fuel rods vibration in a zero-power reactor. The methodology includes uncertainty propagation and sensitivity analysis. The target event is based on an actual experimental campaign at the CROCUS zero-power reactor and corresponds to the simultaneous oscillation of 18 metallic uranium fuel rods in the periphery of the core. Both the uncertainty propagation and the sensitivity analysis commonly use a large part of the entire analysis process, from the selection of uncertain parameters to the actual code simulations. Applying a random sampling-based approach, the input parameters are sampled N times from their distribution information and used as inputs for N noise simulations using CORE SIM +. The quantity of interest (QoI) is the amplitude of the Auto-Power Spectral Density at various detector locations, which is normalized by the amplitude of the Cross-Power Spectral Density of the reference detector. Their uncertainties are determined following the 4th order Wilks' formula for two-sided limits. Through the determination of correlations among QoI at the installed detector locations, it is demonstrated that the neutron noise near the area of oscillating fuel rods (noise source) have different behavior compared to the neutron noise further away from the noise source. The following sensitivity analyses are carried out using multiple correlation coefficients within grouped parameters. As expected from the QoI correlations, the QoIs at two different locations (near and far from the noise source) are influenced by different input parameters. Near the noise source, the QoI uncertainty is driven by the uncertainties in the position of the noise source, while the uncertainties in the nuclear data for U-235 and U-238 are the leading contributors further away from the source. This paper provides general information on how to perform the uncertainty analyses for neutron noise simulations, as well as quantitative estimates of the computational uncertainty required for the validation of the computer programs under development for the simulation of neutron noise.

1. Introduction

Small, stationary neutron flux fluctuations around the expected mean value are known as neutron noise. The need for more extensive research on the neutron noise behavior has arisen in the past few years after unexpected evolution of neutron noise was found in several European power plants. Neutronic noise with magnitudes of up to 10% of the reactor power have been observed in some pressurized water reactors (PWRs) in Europe. In December 2010, the German PWR KKU (Kernkraftwerk Unterweser) went through a sudden increase of the measured neutron flux signal corresponding to 108%FP (Full Power) and this activated the reactor scram (Bundesamt für Strahlenschutz, 2012). Likewise, the Spanish PWR Trillo had to be operated under 93%FP condition to avoid the actuation of the reactor trip by the excessive neutron noise (Almaraz Trillo Report, 2012). These examples represent a clear influence of neutron noise on the plant operations. In this context, the CORTEX (Core Monitoring Techniques and Experimental Validation and Demonstration) project was launched in 2017 in the framework of the EU-Program Horizon 2020 (CORTEX project, 2017). The main aim of CORTEX was to address these challenges by developing an innovative core monitoring technique that allows detecting anomalies in nuclear reactors. The technique is mainly based on using the inherent fluctuations in the neutron flux recorded by in-core and ex-core instrumentation, from which the anomalies can be differentiated depending on their type, location,

* Corresponding author.
E-mail address: demaz@chalmers.se (C. Demazière).

https://doi.org/10.1016/j.anucene.2022.109157
0306-4549/

and physical characteristics. This unfolding is performed using machine learning, for which the training and validation data are provided by simulations of the neutron noise induced by postulated anomalies. In order to investigate the neutron noise behavior under the various conditions more precisely, noise simulators relying on different computational schemes were developed within the framework of the CORTEX project. Accordingly, a series of uncertainty analyses are required to support the validation of the newly developed simulators.

There have been numerous investigations on uncertainty analyses for the nuclear reactor physics applications including criticality and burnup calculations as well as reactor transient calculations (mainly safety related abnormal conditions) (Bostelmann, 2015; Buss et al., 2011; Iwamoto et al., 2018; Rochman, 2016; Zwermann et al., 2014; Hursin, 2018; Bostelmann, 2015), by using dedicated modules and tools such as XSUSA (Zwermann et al., 2014), NUDUNA (Buss et al., 2011), TMC (Rochman, 2011), SANDY (Fiorito, 2016), SAMPLER (which is available with SCALE 6.2) (Rearden, 2015) and SHARK-X (Rochman et al., 2020). However, there has been little attempt to carry out uncertainty analyses under specific neutron noise conditions (the condition belongs to the normal operation of the reactor) in spite of its potential importance on the reactor operation (Yi, 2017; Yi et al., 2018). The works which are described throughout this paper have been conducted under the framework of the CORTEX project. The main objective of this work is to establish a general methodology for uncertainty propagation and sensitivity analysis under specific neutron flux oscillating condition.

The COLIBRI experiment (Lamirand et al., 2016), which involves the periodic movement of fuel rods at the CROCUS zero-power reactor (Lamirand, 2018), as well as its modeling using CORE SIM + (Mylonakis, 2021), are considered as a case study in this paper. The uncertainty of the neutron noise at different detector locations is calculated by considering the individual perturbations of input parameters. Sensitivity analysis is used to determine the input parameters responsible for the output uncertainties.

The paper is organized as follow. First, the experiment as well as the associated computational model are presented in Section 2. Then the overall methodology for uncertainty propagation and sensitivity analysis is presented in Section 3 and its application to the considered COLIBRI experiment is shown in Section 4 and 5.

2. Description of the target experiment

2.1. Target reactor

CROCUS is a research reactor located at the EPFL (École Polytechnique Fédérale de Lausanne) in Switzerland and is selected as the target reactor in this study. CROCUS is a zero-power reactor, with a maximum allowed power of 100W (Lamirand et al., 2016). The core, as shown in Fig. 1, is approximately cylindrical in shape with a diameter of about 60cm and a height of 100cm, while the water tank, where the core is located, is 130cm in diameter. Deionized water (H_2O) acts as both moderator and reflector. There are two different types of fuel rods within the two fuel zones of the core. The central zone is fuelled with uranium dioxide (UO_2) fuel rods and the peripheral zone is loaded with metallic uranium (U_{metal}) fuel rods. The reactivity in the CROCUS reactor is controlled either by the water level using a spillway or by two B_4C absorber control rods.

2.2. Target event

In the experimental campaign at the CROCUS reactor, the vibrating fuel rods experiments have been carried out using the COLIBRI in-core device (CROCUS Oscillator for Lateral Increase Between u-metal Rods and Inner zone) (Lamirand, 2018). The COLIBRI fuel rods oscillator is designed to oscillate simultaneously any of the 18 metallic uranium fuel rods laterally in the west region of the core's peripheral zone. Among the experiments performed, the case with an oscillating amplitude of 2mm and frequency of 1Hz is selected as the target condition in this work. Fig. 1 shows the radial view of the reactor core with the COLIBRI device and the detectors installed. Due to experimental considerations (of detector reliability), the computational uncertainty of QoI related to neutron noise amplitude at the 8 detector locations (Detector 3 $\sim$ Detector 10) is the focus of the present work. The exact formulation of QoI is provided in Section 2.3.4. Even though the uncertainty in the phase of the neutron noise is determined by the uncertainty propagation methodology, its results are not shown here for the sake of conciseness. In the considered case, the spatial variation of the phase is relatively small at the location of the detectors (Vinai, 2021). It was verified that the spatial distribution of the phase uncertainty is also very flat. The developed methodology is nevertheless applicable to the phase of the neutron noise, in case this quantity needs to be examined.

2.3. Description of the computational model and quantities of interest

2.3.1. Noise calculations with CORE SIM+

To list the uncertain parameters to be considered in this work, an overview of the computational scheme used for modeling the experiment is provided. The neutron noise simulator CORE SIM + is based on the two-energy group kinetic neutron diffusion equations and capitalizes on the former experience of the CORE SIM tool (Mylonakis, 2021; Demazière, 2011).

The calculation process consists of two steps: the steady-state neutron flux calculation and the neutron noise calculation in the frequency domain, respectively. CORE SIM + enables modeling the reactor with non-uniform meshes. This feature optimizes the computational cost and especially fits the current target event of "fuel rods vibration", whose noise source is highly localized.

For the modeling of fuel assembly vibrations, the following approach has been selected (Demazière, 2019; Jonsson et al., 2012).

In Fig. 2, three spatially homogenized fuel assemblies are represented, which respectively corresponds to Region I, Region II and Region III and are described by their own sets of macroscopic cross-sections. The assembly in Regions II is assumed to vibrate along the x-axis. Considering Region II and Region III, the spatial distribution of the static macroscopic cross-section for the reaction type α in the energy group g can be represented as.

$$\Sigma^{x}_{\alpha,g}(x) = [1 - \Theta(x-b)]\Sigma_{\alpha,g,II} + \Theta(x-b)\Sigma_{\alpha,g,III}, \tag{1}$$

where $\Theta(x-b)$ is the Heaviside function, i.e.,

$$\begin{cases} \Theta(x-b) = 0 \ if \ x < b \\ \Theta(x-b) = 1 \ if \ x \geq b. \end{cases} \tag{2}$$

Here, we apply the oscillating amplitude $\varepsilon_x(z,t)$, z being the axial coordinate, from b_0 (i.e., the static position of the boundary between Regions II and III), use a first-order Taylor expansion, and change the expression into the frequency domain. The final expression for the noise source becomes.

$$\delta\Sigma^{x}_{\alpha,g}(x,z,\omega) = \varepsilon_x(z,\omega)\delta(x-b_0)\left[\Sigma_{\alpha,g,II} - \Sigma_{\alpha,g,III}\right]. \tag{3}$$

2.3.2. CORE SIM + model of CROCUS

The core is modeled with a three-dimensional mesh of $44 \times 156 \times 54$ cells, in the x-, y-, and z- directions of the core, respectively. The area around the neutron noise source is modeled

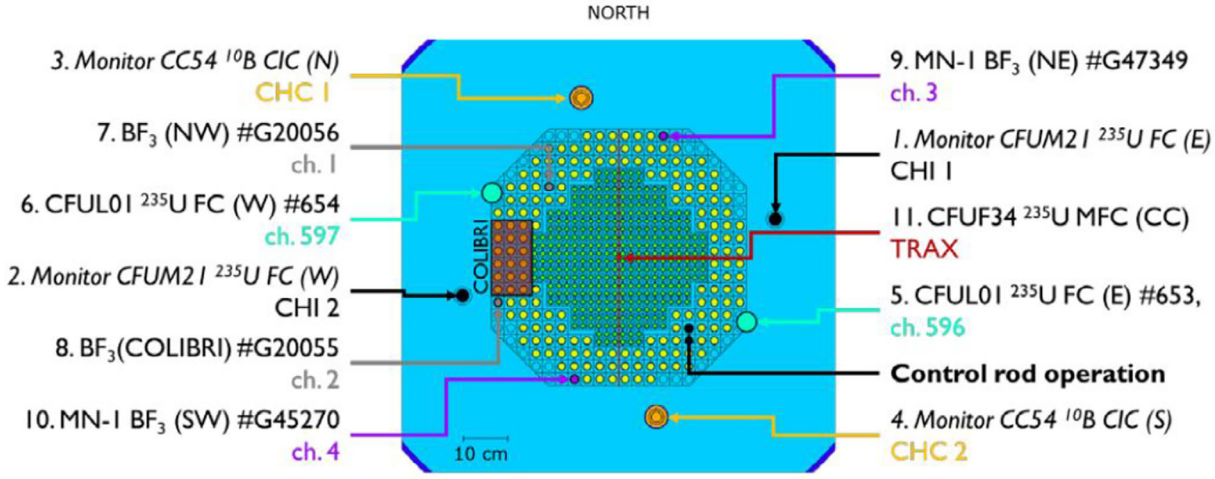

Fig. 1. Radial view of reactor core with the information of installed detectors.

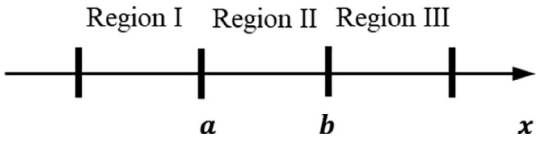

Fig. 2. Representation of three neighboring fuel assemblies with respect to the *x*- direction (Demazière, 2019; Jonsson et al., 2012).

with fine meshes with a size of 2mm, whereas the remaining area is modeled with coarser meshes with a size of 3cm. Fig. 3 shows the modeled reactor core at mid-core elevation.

The two red lines at the boundaries of different regions represent the location where the noise sources are assigned for the noise simulation[1]. The homogenized nuclear data are assigned to the corresponding meshes of the model through a MATLAB script developed in the course of this work.

2.3.3. Homogenized group constant with Serpent

The Serpent model of the CROCUS reactor has been built specifically for cross-section generation purposes (Rais, 2017). The two-energy group cross-sections are generated with Serpent v2.1.30 for 8 universes in the reactor core: four in the radial direction (UO_2 region, U_{metal} region, control rods region and reflector region, as described in Fig. 4 (Rais, 2018) and two in the axial direction (regions under and above the water level). The calculation is performed using the JEFF-3.1.1 nuclear data base, with 150 active cycles of $5{\cdot}10^5$ source neutrons, skipping the first 100 cycles. At the same time, the effective kinetic parameters for the equivalent reactor conditions are generated through the Serpent computation (Leppänen et al., 2014).

2.3.4. Nominal neutron noise distribution

In the experiments carried out within the CORTEX project, the detector time series are converted into the frequency domain for the purpose of validating the noise simulators (Mylonakis, 2021). The conversion is made through the Fourier transform of auto- and cross-correlation functions. These are the so-called APSD (Auto-Power Spectral Density) and CPSD (Cross-Power Spectral Density), which are defined as (Newland, 2012);

$$APSD(f) = \int_{-\infty}^{\infty} C_{xx}(\tau) e^{-j2\pi f\tau} d\tau \tag{4}$$

$$CPSD(f) = \int_{-\infty}^{\infty} C_{xy}(\tau) e^{-j2\pi f\tau} d\tau,$$

where τ is the lag used to estimate the autocorrelation function of the sensor output signal and C_{xx} and C_{xy} are calculated with Equation (5).

$$C_{xx}(\tau) = E[x(\tau)x(t+\tau)] \tag{5}$$

$$C_{xy}(\tau) = E[x(\tau)y(t+\tau)]$$

The obtained APSD amplitude for the considered detector is normalized by the CPSD amplitude of the same detector and the reference Detector 5; this is the quantity of interest (QoI) used in the CORTEX project (Hursin, 2021).

When using CORE SIM+, the APSD and CPSD are derived from the static neutron flux (ϕ_0) and the neutron noise ($\delta\phi$) at the locations of the detectors (i) following the equations below (Mylonakis, 2021).

$$APSD_i = \left(\frac{\delta\phi}{\phi_0}\right)_i \left(\frac{\delta\phi}{\phi_0}\right)_i^{\dagger} \tag{6}$$

$$CPSD_{i,j} = \left(\frac{\delta\phi}{\phi_0}\right)_i \left(\frac{\delta\phi}{\phi_0}\right)_j^{\dagger},$$

where † symbolizes the complex conjugate and j indicates the reference detector.

Fig. 5 shows the spatial distribution of the thermal neutron noise at mid-height of the core, in nominal conditions where all input parameters take their nominal values and no uncertainty is considered (see Table 1), for two different quantities: the absolute noise amplitude and the QoI amplitude.

The absolute noise amplitude describes the magnitude of the neutron noise, which is directly converted from the original complex quantity obtained from the CORE SIM + computation.

Compared to the absolute (original) noise whose behavior is following the pattern of the fundamental flux, as shown in Fig. 5-a, the QoI magnifies the spatial component of the neutron noise as compared to the point-kinetic component.

[1] The modeled oscillating boundary which is closer to the core center (right-side red line in Fig. 3) is shorter than the left side boundary although the actual two boundaries have same length as shown in Fig. 1. This is because CORE SIM+ builds the noise source associated with the vibration from the differences between the cross-sections of the regions on the left and on the right sides of the moving boundaries (see Equation (3)). Thus, the parts of the moving boundaries that are between regions with the same cross-sections are not shown since their perturbation is zero.

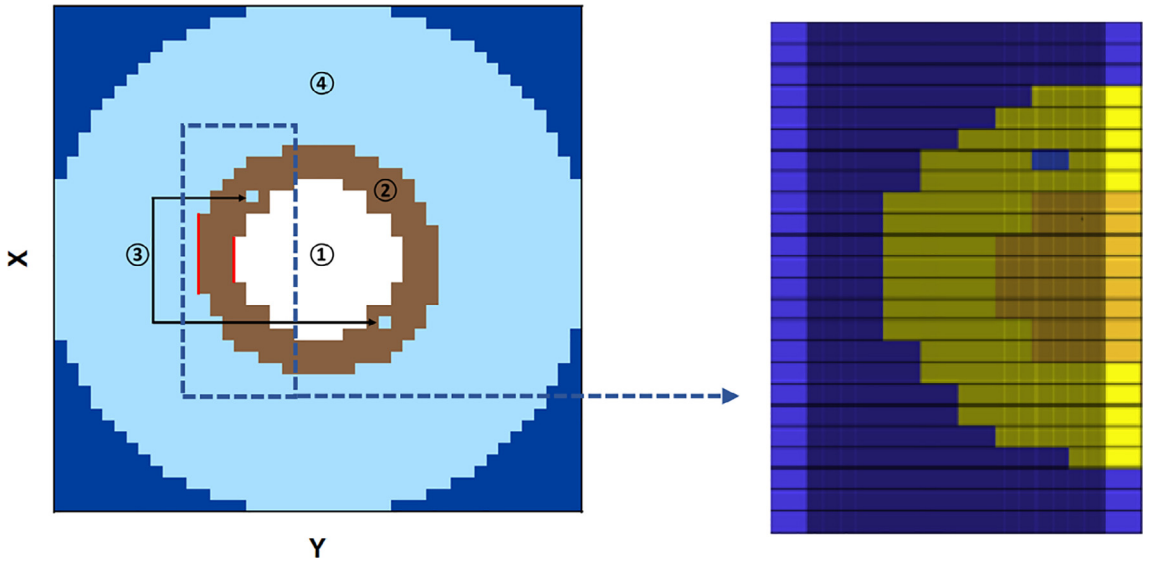

Fig. 3. Modeled reactor core in CORE SIM+ (left) and the area around oscillating fuel rods modeled with fine meshes (right) (①: Central zone with UO_2, ②: Peripheral zone with U_{metal}, ③: Control rods, ④: Reflector).

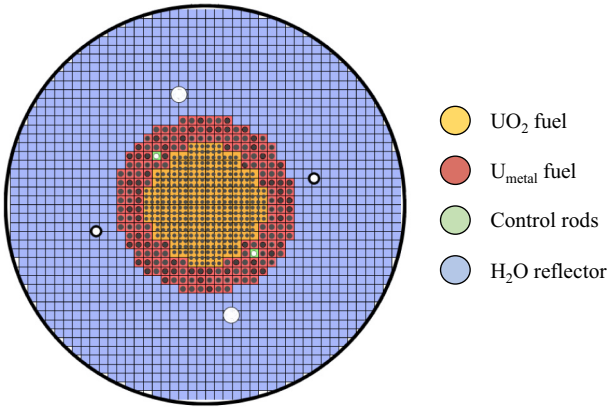

Fig. 4. Radial nodalization for the region of the core.

3. Uncertainty propagation and sensitivity analysis with CORE SIM+

For uncertainty quantification, there are two main approaches available, namely the deterministic method and the stochastic sampling-based method (Zhu, 2015; Zhu et al., 2015). The deterministic method, colloquially known as the "Sandwich Rule" method, computes first-order sensitivity coefficients of the output parameters of interest and then combines the sensitivities with the covariance matrix of the input data. The stochastic sampling-based method is based on the perturbation of the uncertain input data as random variables following their uncertainty distributions. The variance of the output parameter corresponds to the contributions of the input parameters' uncertainty. Among these two approaches, the stochastic sampling-based method is selected due to its advantages in the current work. This method involves the straightforward implementation and implicit treatment of the non-linearity of the model by computing the output uncertainty through the simultaneous consideration of all input uncertainties. Moreover, different from the deterministic method, the

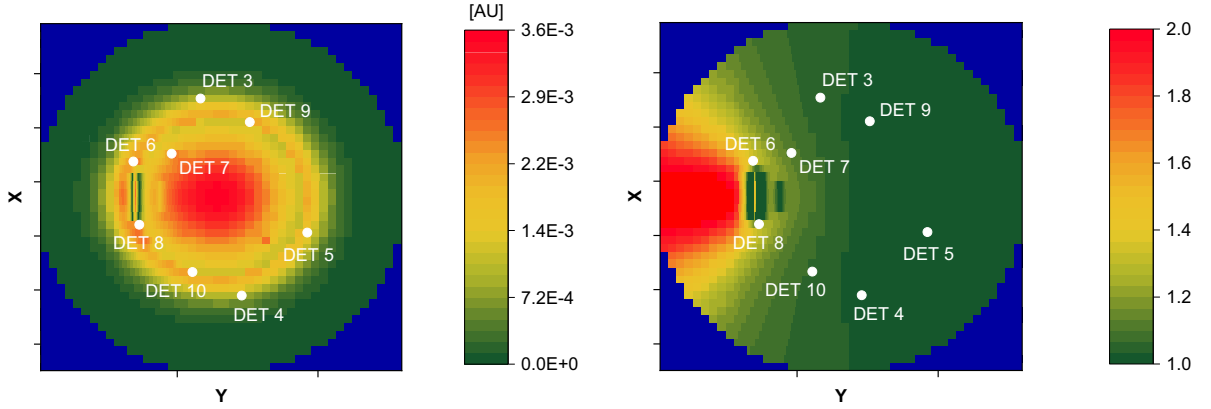

a. Absolute noise amplitude

b. APSD amplitude normalized by CPSD at the Detector 5 location (QoI)

Fig. 5. Thermal neutron noise behavior in the mid-height of the core.

Table 1
Probability distributions associated with the selected uncertain parameters.

No.	Parameter		Distribution	Unit	Nominal value	Standard deviation (Lower/Upper limit[a]) (Dependent parameter[b])
1	Water level		Normal	cm	95.22	0.01
2	Initial pool temperature		Normal	°C	20.0	0.02
3	Initial pool density		–	g/cm^3		<2>
4	Fuel density	UO_2	Normal	g/cm^3	10.556	0.034
5		U_{metal}	Normal	g/cm^3	18.677	0.044
6	Nuclide mass fraction	U-235 of UO_2	Normal	–	1.806E-2	7E-6
7		U-238 of UO_2	–	–		<6>
8		U-235 of U_{metal}	Normal	–	9.470E-3	7E-6
9		U-238 of U_{metal}	–	–		<8>
10	Active fuel length		Normal	cm	100.0	0.02
11	Relative axial location	Bottom of upper Grid	–	cm		<10>
12		Bottom of upper Cd	–	cm		<10>
13		Top of upper Cd	–	cm		<10>
14		Top of upper Grid	–	cm		<10>
15		Fuel rod top spring	–	cm		<10>
16	Fuel diameter	Fuel rod outer surface of UO_2	Normal	cm	0.526	8.5E-4
17		Cladding outer surface of UO_2	Normal	cm	0.63	5E-3
18		Fuel rod outer surface of U_{metal}	Normal	cm	0.85	1E-3
19		Cladding outer surface of U_{metal}	Uniform	cm	0.965	0.965 / 0.97
20	Cladding thickness	UO_2	Normal	cm	0.085	5E-3
21		U_{metal}	Normal	cm	0.1	5E-3
22	Inner surface of cladding	UO_2	–	cm		<17>, <20>
23		U_{metal}	–	cm		<19>, <21>
24	Square pitch	UO_2	Normal	cm	1.837	2E-4
25		U_{metal}	Normal	cm	2.917	2E-4
26~773	Nuclear data uncertainties[c]					
774	Oscillating amplitude		Normal	cm	0.2	0.01
775	Oscillating frequency		Normal	Hz	1	0.05
776	Location of noise source		Uniform	Mesh	Ideal oscillating boundary	−1/+1

[a] This column shows the value of lower and upper limit in case of having uniform distribution.
[b] This column shows the correlated parameters which are composing the corresponding parameter in case of having no specific distribution information (<***k***> represents the parameter consistently with the ID numbers given in the first column).
[c] Nuclear data uncertainties are treated in a distinct manner and detailed information on this treatment is described in Section 3.2.

stochastic sampling-based method does not require an earlier computation of sensitivity coefficients for the uncertainty quantification. Therefore, this approach becomes suitable, especially for involving the perturbation of the complicated groupwise nuclear data and enhances the accuracy of the obtained neutron noise uncertainties.

Fig. 6 shows a schematic flow chart of the developed methodology, including the expected outcomes from each step. The subsections below describe the important points involved in the various steps.

3.1. Listing uncertain parameters

The neutron noise balance equation implemented in CORE SIM + is written in a compact form as reported below (Cacuci, 2010).

$$\boldsymbol{L}\delta\phi = \delta S, \tag{7}$$

where $\boldsymbol{L}$ is the diffusion approximation of the transport operator, which depends on the neutron diffusion coefficients, the kinetics parameters, the effective multiplication factor of the system and the static cross-sections of the system. The noise source term, δS, refers to the neutron noise source resulting from the fluctuations of the cross-sections as described in the former section.

In this work, a number of input parameters that can influence the behavior of the target reactor and the event are investigated. They are selected based on expert judgement (see Table 1 the "Parameter" column). For $\boldsymbol{L}$, the uncertainties in the design and operating parameters and the nuclear data can be considered as influential and possibly correlated parameters (Kasemeyer, 2007). Meanwhile, the parameters related to the static cross-sections are already considered as one of the components in $\boldsymbol{L}$, which determines the fluctuation of the macroscopic cross-sections influencing the noise source as modeled in Equation (3). Therefore, the oscillating amplitude, the oscillating frequency, and the exact location of the noise source can be considered as the factors influencing the noise source (δS). Table 1 summarizes the selected 776 parameters with their distribution information. Here, 748 nuclear data uncertainties are perturbed as described in Section 3.2. Additionally, 10 of the 28 remaining parameters are correlated and sampled accordingly, while the remaining 18 parameters are sampled independently. Since the location of the noise source can only be perturbed within a discrete number of meshes, it is designed to be perturbed with three values along the oscillating direction, −1, 0 and + 1: −1 signifies the movement of 1 mesh away from the core center, while + 1 means the movement of 1 mesh towards the center.

3.2. Generation of random samples

Random sets of perturbed input parameters are generated based on the distribution information with a Simple Random Sampling (SRS) method using a specifically designed MATLAB script. The eventual correlations are taken into account. The resulting input data sets are then used in a series of computations with Serpent in order to create the sets of two-energy group macroscopic cross-sections needed for the CORE SIM + calculations.

The sampling of nuclear data, needed for generating group constants uncertainties, deserves further explanation, as it usually involves many correlated inputs. The generation of the perturbed set of nuclear data is done through the sampling of multigroup covariances by using the Paul Scherrer Institute (PSI) tool "NUSS (Nuclear data Uncertainty Stochastic Sampling)" (Zhu et al.,

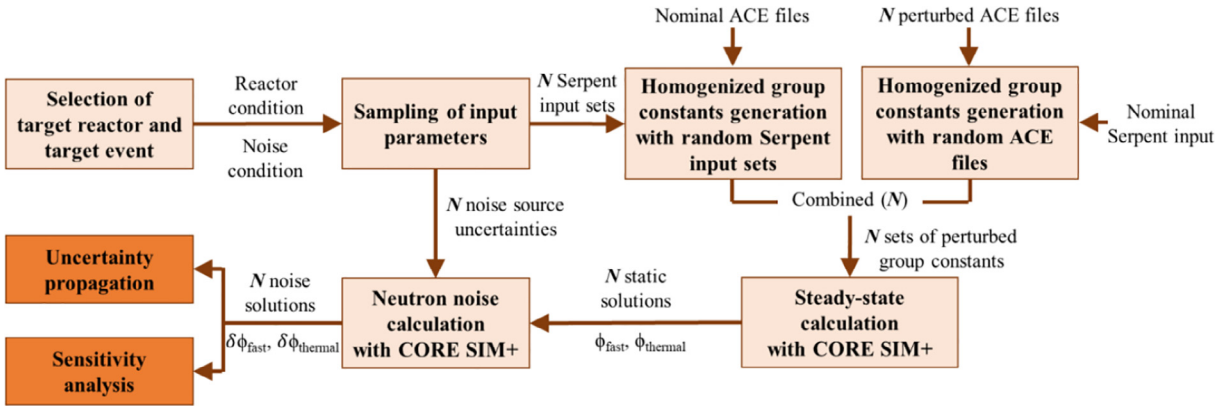

Fig. 6. Flow chart for the uncertainty analyses.

2015). NUSS is used in the present work to generate a perturbed set of the ACE formatted file, which will be used in the Serpent calculations required to produce the random sets of two-group constants needed for CORE SIM +. The Serpent calculations were performed with Serpent v2.1.29, using its native ENDF/B-VII.0 ACE files and ENDF/B-VII.1 covariances and the Scale 6.0 energy group structure (Hursin, 2020). The microscopic data for U-235, U-238, H-1 and O-16 are considered while the following reaction types are perturbed: (n, el), (n, inl), (n, 2n), (n, capture), (n, f), $\bar{\nu}$ and χ. The relevant propagated nuclear data consist of diffusion coefficient (D), absorption cross-section (Σ_{abs}), nu-fission cross-section ($\nu\Sigma_{fiss}$), and removal cross-section (Σ_{rem}) of two-energy groups in 8 reactor core regions as described in Section 2.3.3.

It should be noted that, even though the kinetic parameters are perturbed in CORE SIM+, their uncertainties do not include uncertainties in their physical values, only the effect of nuclear data perturbations on the effective quantities determined by Serpent.

A total of 300 input sets are generated for the statistical uncertainty propagation using CORE SIM+, a batch computation with CORE SIM + is performed for both static and dynamic reactor conditions. Since CORE SIM + performs the calculations in the frequency domain, the obtained neutron noise is a complex quantity, with an amplitude and a phase. The QoI in this work are post-processed accordingly (see Equation (6)).

3.3. The methodology of uncertainty propagation

A series of uncertainty propagation calculations have been performed that yield tolerance limits determined by the Wilks' formula using the GRS (Gesellschaft für Anlagen und Reaktorsicherheit) methodology (Kloos and Hofer, 1999). This methodology is a non-parametric statistical method based on well-established concepts of probability and statistics theory. The number of necessary code calculations, which corresponds to the size of the output sample, depends on the requested probability content and confidence level of the tolerance limits used to express the uncertainty of the output results. These extremes of the intervals are the estimates of the quantiles of the actual unknown probability distributions of the results, which statistically quantify their uncertainty. In this respect, this approach requires a relatively small number of actual code runs. Additionally, it saves the computational cost compared to that of brute force Monte Carlo methods which can determine the actual probability distribution of the output uncertainty within specific confidence level. In this latter case the determination of these probability distributions with a level of statistical confidence of 95% usually requires hundreds or thousands of code executions.

Following the U.S.NRC regulatory guide 1.105, it is recommended to use 95%/95% tolerance limits for quantifying uncertainties in code results (U.S. NRC, 1999). In addition, one of the previous uncertainty studies for best-estimate nuclear system codes, the BEMUSE analysis of the LOFT L2-5 test, indicated that applying the Wilks' formula to the 4th or 5th order usually produced a more precise tolerance interval— considering 4th or 5th order makes statistically better estimation of the actual 5%–95% quantiles of the output's probability distribution, at the price of some additional code executions (Reventós, 2008). Thus, the 4th order Wilks' formula for two-sided tolerance limits is considered for the analyses reported hereafter. The main reason for choosing the two-sided tolerance limits in the analyses is that the obtained results will be used in the validation process of the neutron noise simulator. Therefore, both upper and lower limits matter for the comparison with the equivalent experimental results. For the 4th order Wilks' formula for two-sided limits, a total 260 output samples are required from the code runs (Porter, 2019). Among the ranked output results, the 4th largest and the 4th smallest values statistically guarantee the uncertainty propagation result to satisfy the 95%/95% criterion, 95% of probability content in the interval (output variability), with a 95% of confidence that this is true.

3.4. The methodology of sensitivity analysis

Owing to the complexity of the physical processes driving the neutron noise behavior, a variance-based approach for sensitivity analysis has been considered for the neutron flux oscillations in order to obtain more precise results (Yum, 2019). Variational methods are well suited to deal with linear and non-linear phenomena in the solution of differential equations and can be applied to the general time-dependent neutron diffusion equations with thermal–hydraulic feedback in the neutronic data. CORE SIM+, however, solves the linearized neutron oscillation problem in the frequency domain without considering any thermal–hydraulic feedback. The second-order perturbation terms are neglected and as such all possible induced non-linearities in the solution of the neutron noise equations (Demazière, 2011). This simplifies the mathematical treatment without significantly affecting the physical accuracy in the case of weak non-linear effects. This linear approximation allows us to consider other statistically based approaches for sensitivity analysis, which avoids the need to modify the code to introduce the variational techniques mentioned above e.g., regression or correlation-based approaches. Therefore, the Pearson's correlation coefficient (PCC) and the Spearman's rank correlation coefficient (SCC) are selected for sensitivity measures because of their simplicity and ease of use. The compatibility of these two coefficients is discussed later to confirm the validity of

PCC based sensitivity index in noise calculations. These coefficients only require the condition of the data without bifurcations or sudden discontinuities, which are not expected on neutron noise analysis[2]. The PCC is a measure of linear correlation between two sets of data, whose value corresponds to the covariance of two variables, divided by the product of their standard deviations (Conover, 1980; Kent State University, 2021). The SCC is a non-parametric measure of rank correlation and provides information on how well the relationship between two variables can be described using a monotonic function (Conover, 1980).

Additionally, it is necessary to set up a clear criterion that allows to discriminate the meaningful values of a correlation coefficient according to a critical value. This can be done by using a test statistic for the null hypothesis that there is no correlation between two variables depending on the considered sample size. (Ramsey, 1989). Here, we set a significance level, which is a threshold of probability depending on whether we accept or reject our null hypothesis. Following a general guideline, it is taken as 5%, and lastly, the critical value is obtained as 0.06 with a sample size of 1000 by using the Z test (Ramsey, 1989; Kajuri, 2018). This means that, if the absolute value of the calculated PCC or SCC based on 1000 samples is larger than 0.06, we can regard that the input and output variables are "correlated" with a 5% probability that this correlation is not true, that is, a level of confidence of 95%.

As a last step, the calculated coefficient is squared to represent the "sensitivity index", which expresses what fraction of the variation of dependent variable is explained by the variation in the independent variable (Bluman, 2009).

Due to the fact that nuclear data input parameters are both numerous and correlated, a methodology is adopted to measure the effect of large number of correlated input parameters efficiently (Hursin, 2018), through the determination of a correlation coefficient for a group of input parameters. The multiple correlation coefficient of a group, denoted here as group 1 ($X_{(1)} = (X_1, \cdots, X_k)$), is calculated following the equation below.

$$R^2_{(1)} = (r_p(Y,X_1), \cdots, r_p(Y,X_k))\Sigma^{-1}_{X_{(1)}}(r_p(Y,X_1), \cdots, r_p(Y,X_k))^T, \quad (8)$$

where $r_p(Y,X_i)$ is the correlation coefficient between Y and X_i, and $\sum^{-1}_{X_{(1)}}$ is the inverse of the variance–covariance matrix (VCM). The multiple correlation coefficient $R^2_{(1)}$ can be used to represent the first order sensitivity index for a group of parameters,

$$S_{(1)} = R^2_{(1)}. \quad (9)$$

In Section 5.2, the input parameters are divided in three groups which are not correlated among each other. Group 1 is composed of all the nuclear data parameters. It is referred to as "group of nuclear data" later on. Group 2 consists of the parameters related to the reactor design and operation (parameters no.1 to no. 25 listed in Table 1) and is named as "group of design and operating parameters". Groups 3 is made up of the input parameters related to the description of the noise source (parameters no. 774 to no. 776 in Table 1) and referred to as "group of noise source data". The relative contributions of three groups are compared through the two different approaches in the following sensitivity analysis: the main focus of the first approach is to compare the QoI uncertainties at the detector locations perturbing one group of input parameters at a time. The second approach, however, measures the exact amount of contribution of each group to the neutron noise by means of the sensitivity index.

[2] One input parameter named "location of noise source" perturbs within discrete values due to the nature of CORE SIM+ model. However, this parameter is continuous in nature, thus, sampling within discrete values should not impact on predicting a linear correlation with output variable.

4. Outcome of the uncertainty propagation applied to the COLIBRI experiment in CROCUS

Based on 300 output samples, the radial distribution of QoI uncertainties is analyzed to gain a better understanding of its spatial variation, especially with respect to the distance to the noise source. Next, the QoI uncertainties at the detector locations are analyzed. This analysis involves an investigation of correlated behavior among the QoIs at the detector locations. Additionally, the influence of the Monte Carlo uncertainty on the QoI uncertainties is considered. Finally, the linearity of the current calculational scheme is investigated using the distribution characteristics of the output samples.

4.1. Uncertainties associated to the induced neutron noise

In order to gain an overview of the output variability, its values in the radial direction of the core have been determined at the core mid-height, where all the detectors are installed, and the results are depicted in Fig. 7. This map is obtained from 260 radial maps of the QoIs, whose number corresponds to the required number of code runs for the 4th order Wilks' formula for two-sided limits. The 260 outputs are extracted randomly from the 300 simulated cases. The value at the specific local point is calculated as follows: first, the QoIs at this location from the prepared 260 radial maps are extracted. Second, the difference between the 4th largest and the 4th smallest among these 260 values is calculated. Third, this difference value is normalized by the mean value of 260 data at this local point.

The uncertainty is highly localized in the area of the oscillating fuel rods. With the exception of this area, the magnitude of the uncertainty is lower throughout the core, while the neighboring area of the oscillating fuel rods still shows a larger uncertainty than the remaining core area. This separation of the reactor core into two regions (neighboring area of the noise source and the rest) can also be observed in the correlations between the neutron noise calculated at the detector locations shown in Fig. 8. This figure represents a correlation matrix for the QoIs at the different detector locations based on 300 random outputs. Detectors 6 and 8, which are closest to the noise source, are strongly correlated together and less correlated to the others. The other detectors are also very strongly correlated among each other.

Fig. 9 compares the QoI uncertainties between the simulation results and the actual experimental results from the first experimental campaign performed with the COLIBRI device (Lamirand, 2020). Two simulation cases are presented, i.e., the case that propagates both the uncertainties associated with the 776 input parameters in Table 1 and the statistical error of the Monte Carlo estimation of the nuclear data, and the case that takes only into account the Monte Carlo statistical error of the nuclear data.

At all detector locations, the experimental uncertainties are much larger than the computational uncertainties in general. The statistical uncertainty shown in Fig. 9 results from the Monte Carlo nature of the two-energy group cross-sections generation process performed with Serpent. The uncertainties of noise amplitude with and without considering the uncertain parameters (as listed in Table 1) are compared in this figure. Only the statistical uncertainty from the Serpent computation is included in the case of "with statistical uncertainty". In all detector locations in Fig. 9, the uncertainties of neutron noise involving the perturbation of uncertain parameters is around 100 times larger than those calculated without uncertain parameters. Therefore, the statistical uncertainty stemming from the Monte Carlo simulations themselves is confirmed as negligible and will not be discussed further in this paper.

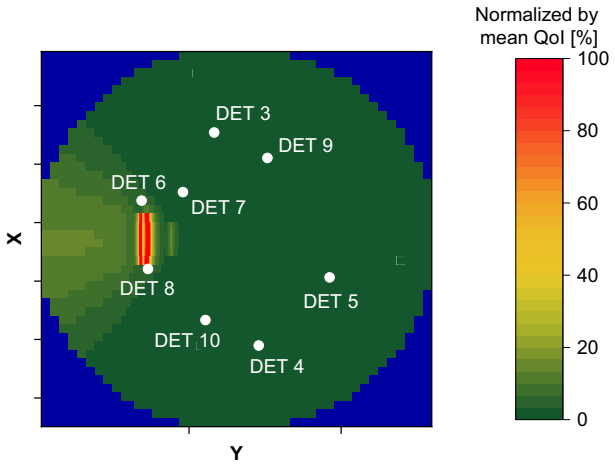

Fig. 7. Radial distribution of the relative QoI uncertainty (at mid-height).

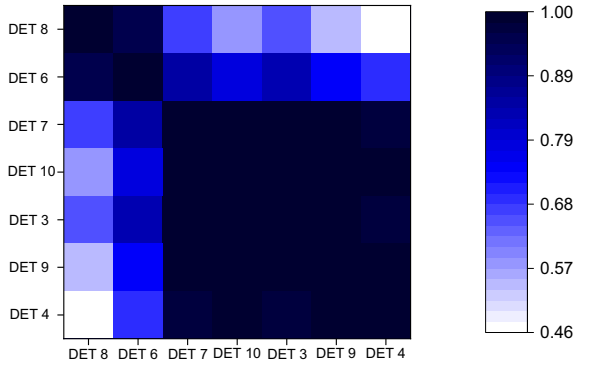

Fig. 8. The correlated behavior among the QoIs at the detector locations.

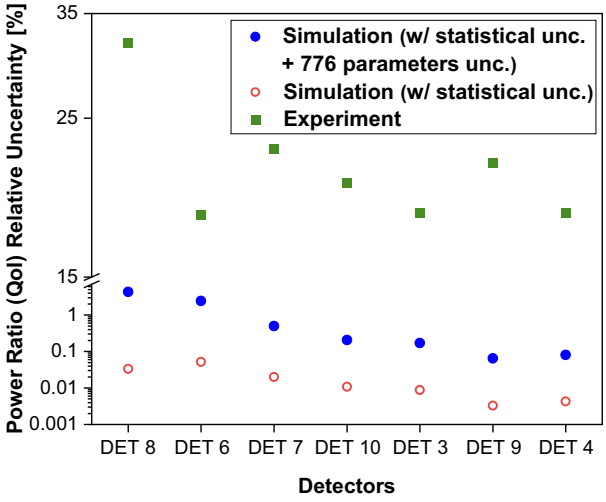

Fig. 9. Comparison of the QoI uncertainties.

4.2. Distribution of the considered responses

Additionally, the distribution information of 300 neutron noise simulations (the absolute noise and the QoI) is collected to investigate the linearity of the current calculational scheme when propagating uncertainties. In this respect, a series of normality tests are performed with the Shapiro-Wilks approach (Shapiro and Wilk, 1965), considering as output samples, the real and imaginary part of the absolute noise and the QoIs at the detector locations. Table 2 summarizes the obtained p-values. A linear approximation for the solution of the neutron noise balance equations is implemented in CORE SIM+, which neglects second-order perturbation terms for the neutron noise (Mylonakis, 2021). There is nevertheless a non-linearity in the noise source, when both the uncertainty in the amplitude of the displacement and the uncertainties in the static cross-sections are considered, as Equation (3) demonstrates. Since the current study considers both uncertainties, there is a possibility that the calculation process of absolute neutron noise becomes non-linear. Meanwhile, by nature, the APSD and CPSD involve the product of two complex numbers as described in Equation (6), and, as such, are non-linear functions of the neutron noise.

In Table 2, both real and imaginary parts of the absolute noise are confirmed as having large p-values, which validates the normality of the data. Since most input parameters have a normal distribution as described in Table 1, the output data is also expected to be characterized by a normal distribution if it results from a linear combination of the inputs. The large p-values suggest indeed that the simultaneous perturbation of the "amplitude of the displacement" and the "static cross-sections" does not result in any significant non-linearity. The following sensitivity analysis (in Section 5) will confirm that this assumption is correct. On the other hand, the QoIs have smaller p-values in general due to the conversion process from the absolute noise to the APSD and CPSD, which are non-linear.

Confirming the linearity between inputs and outputs when propagating uncertainty plays a key role in choosing a proper approach for the sensitivity analysis (e.g., the possibility of using PCC). The compatibility of the different approaches for the sensitivity analysis is discussed later in Section 5.2.2, to identify and choose the most appropriate direction for further analysis.

Next, we investigate what the main contributors to the considered response uncertainty are.

5. Sensitivity analysis of the CROCUS experiment

This section consists of three parts. In the first part, the convergence of sensitivity indices with different sample sizes is investigated in order to determine the minimum sample size required for a reliable quantitative estimate of the sensitivity indices. The other two parts refer to the main sensitivity analyses using two different approaches. The first one is a simplified approach which ranks the parameters by means of the QoI uncertainties propagated by perturbing three different groups of input parameters introduced in Section 3.4 separately. In the second approach, the exact level of contribution of the input parameters is measured by calculating the sensitivity indices. This process involves a calculation of multiple correlation coefficients within the grouped parameters to perform a groupwise sensitivity analysis. Accordingly, the most influential group (group of parameters or individual parameters) for the different detector locations is identified.

5.1. Convergence of the sensitivity indices with the number of samples

A series of convergence tests with different sample sizes are performed to define the proper sample size for further analyses which guarantees the "convergence". Here, "convergence" means that the sensitivity index is similar across replications under the same sample size by using a bootstrap approach (Hsieh et al., 2018). The sensitivity indices considered for the convergence assessment are calculated between two input parameters and the QoI at the location of Detector 8. Parameters with a small (U-238

Table 2
p-values of the neutron noise calculated from Shapiro-Wilks test.

Parameter	p-value						
	DET 8	DET 6	DET 7	DET 10	DET 3	DET 9	DET 4
Real part	0.45	0.72	0.82	0.93	0.82	0.93	0.82
Imaginary part	0.49	0.76	0.27	0.53	0.60	0.53	0.61
QoI	1E-13	1E-5	0.18	0.29	0.19	0.33	0.35

elastic scattering cross-section of energy-group 9) and large sensitivity (location of noise source) are chosen to cover all possible convergence behavior. The tests are carried out with different sample sizes between 10 and 1000, which are sampled randomly from 1000 existing data sets. The sampling of equivalent sample size is repeated 1000 times using bootstrapping with replacement (Sarrazin et al., 2016). Afterwards, to compute 95% confidence intervals, the 2.5th and 97.5th percentiles of the index distribution (1000 indices at each sample size) obtained by bootstrapping are identified. The sensitivity indices and their confidence intervals at different sample size are given by the convergence plots in Fig. 10.

The confidence intervals decrease as the sample size increases. When the sample size is larger than 600, a difference between the calculated confidence interval (with a sample size larger than 600) and the final estimation with 1000 samples becomes smaller than 0.01. Considering the small difference with the final estimation, further analyses using more than 600 samples are deemed sufficiently converged.

5.2. Sensitivity analyses at the detector locations

5.2.1. Simplified approach for parameter ranking

The relative effects of the different groups of parameters (namely, group of design/operating parameters, group of nuclear data and group of noise source data) are investigated by comparing the uncertainties propagated from the different groups as shown in Fig. 11. The uncertainties are obtained following a 1st order Wilks' formula for two-sided limits to reduce the number of samples and consequently the computational cost of such analysis. As the main objective of this study is a qualitative ranking of the groups, the use of a lower order Wilks' formula is acceptable.

The effect of the group of design and operating parameters is confirmed as negligible for all detector locations. At the detector locations near the noise source (Detectors 8 and 6), the QoI uncertainties are mainly driven by the group of noise source data and the group of nuclear data. When the detector is located further away from the noise source, only the group of nuclear data is influential.

5.2.2. Analysis using groupwise sensitivity indices

The uncertainty due to the group of design and operating input parameters is excluded from now on due to its negligible effect as confirmed in Fig. 11. The approach described in Section 3.4 is used to calculate the multiple correlation coefficients of the groups. This requires an estimation of the correlation among the parameters belonging to a same group (see Equation (8)). In this study, the analysis using groupwise sensitivity indices is repeated twice with different grouped parameters. The first trial is carried out with two groups: the group of nuclear data and the group of noise source data. In the second analysis, the group of nuclear data is subdivided into four nuclide groups (all nuclide reaction pair of a given nuclide are grouped together) while the group of noise source data is separated into three individual parameters (oscillating amplitude, oscillating frequency and location of noise source). Additionally, this calculation scheme using a multiple correlation coefficient requires a large number of samples, hence, a sample size of 1000 is considered in this section.

Meanwhile, despite of its suitability in the current calculational scheme, the PCC might not provide significant information since the input and output (QoI) parameters considered in this study are not linearly related. Therefore, the applicability of the PCC in the current analysis condition is discussed in the following section.

1) Assessment of Pearson correlation coefficient

Current work handles a large number of input parameters, where an analysis with grouping input parameters can be efficient especially when the parameters are correlated. A sensitivity analysis with grouping parameters requires a use of PCC as introduced in Section 3.4.

In order to use PCC, a "linear model" between the output data and input parameters belonging to a same group should be guaranteed. However, the output data in this study (QoI) is the APSD amplitude normalized by the CPSD amplitude at the reference detector location, whose calculation process is non-linear but monotonous as confirmed in Table 2. Under these circumstances, a series of tests are carried out to confirm whether the PCC can be still used as a sensitivity measure between input parameters and QoI.

These tests are conducted by comparing PCC and SCC[3] calculated between inputs and two different output data which are the results from "linear" and "non-linear" processes. A good agreement in between can ultimately assure an applicability of PCC to a current sensitivity analysis with grouping parameters. The first calculation involves linearly related input and output parameters, for which PCC should be an accurate measure of sensitivity. The next calculation involves input and output parameters, which are not linearly related. It is intended to check that the PCC can provide the proper input ranking. According to the normality test introduced in Table 2, the output data from the linear and non-linear processes correspond to the absolute neutron noise (real and imaginary parts) and the QoI, respectively.

Fig. 12 compares the results from two different approaches for three different output data at the location of Detector 8.

There is no strong dispersion around the line $y = x$ in Fig. 12 for both outputs. It can be concluded that the PCC produces reliable sensitivity indices for both absolute noise and QoI. Therefore, the PCC is used for ranking the importance of the input parameters (both individual parameters and grouped parameters).

2) Estimation of groupwise sensitivity indices

The sensitivity indices of two groups (group of nuclear data and group of noise source data) for different detector locations are shown in Fig. 13-a. A similarity with the results from the simplified approach (see Fig. 11) can be found, in terms of the level of

[3] The SCC relies on the correlation between the "rank values" of two parameters (Conover, 1980). Therefore, it can detect the monotonic relationship (linear or non-linear) between the parameters and can be used to verify that the PCC provides a reasonable measure of sensitivity even with a non-linear model.

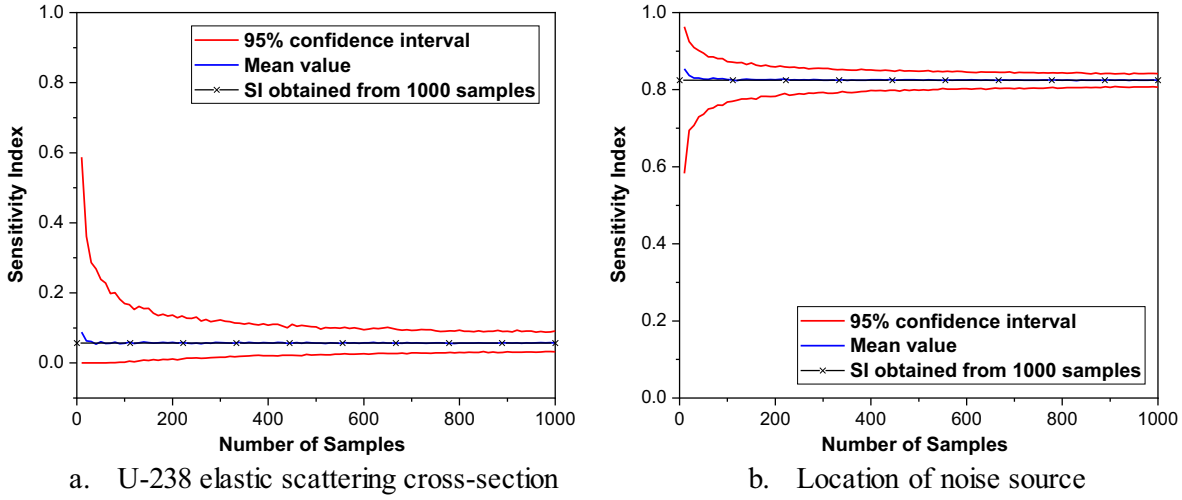

Fig. 10. Convergence plots of sensitivity indices with 95% confidence intervals ("SI" denotes "sensitivity index".).

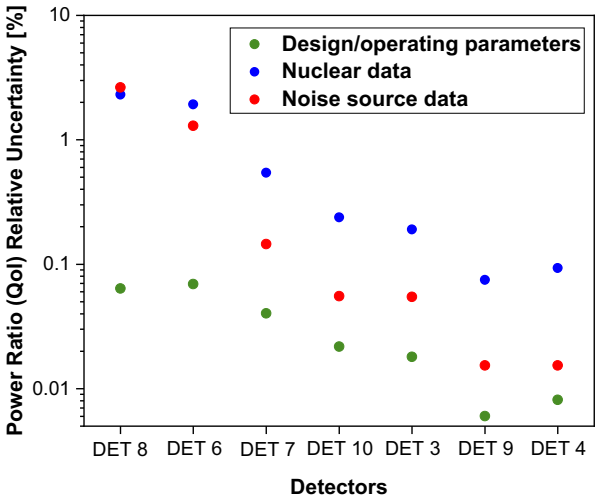

Fig. 11. Comparison of neutron noise uncertainties obtained from the different groups of input parameters.

contribution of each group at different detector locations. The group of noise source data dominates at the locations close to the noise source. However, its effect becomes negligible as the detector location gets further away from the noise source and the group of nuclear data becomes dominant instead. Meanwhile, considering that the sensitivity index here is identical to the first order sensitivity indices (see Equation (9)), the sum of sensitivity indices of two different groups is expected to become unity when they are uncorrelated with each other. However, the actual sums of the results shown in Fig. 13 are larger than 1.0 at all detector locations. This is due to the low number of samples ($n = 1000$) considered here, which does not allow a faithful representation of the covariance matrix in Equation (8).

To support this statement, a series of sensitivity tests with different samples sizes are carried out. Fig. 14 represents the sensitivity indices of two groups at the location of Detector 8, which vary with the sample size. In case of "Group of noise source data", the sensitivity index as well as the confidence intervals converge quickly with the increasing number of samples. On the other hand, the sensitivity index of "Group of nuclear data" decreases gradually, while the confidence interval remains constant. Since only

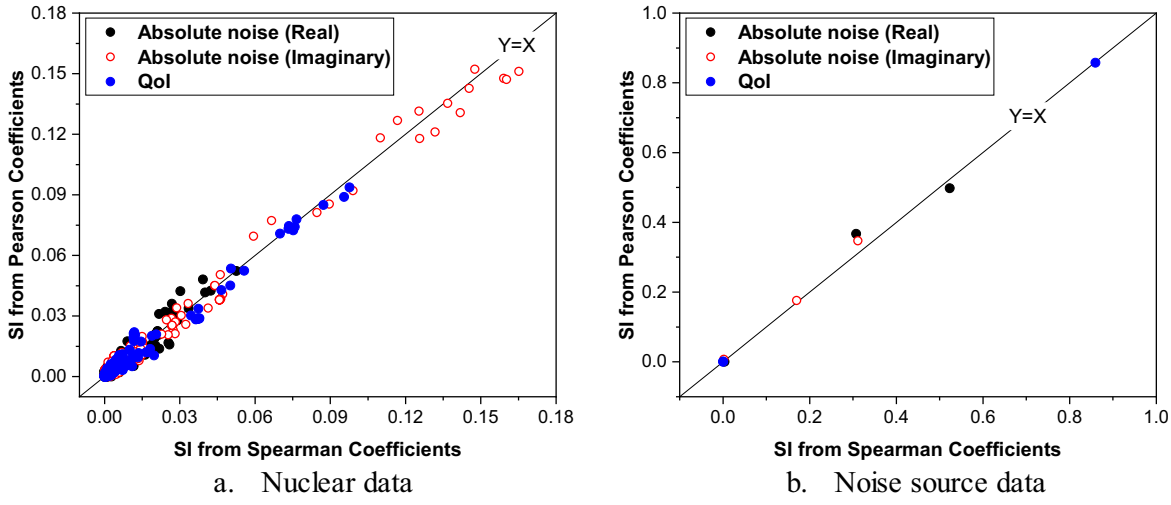

Fig. 12. The comparison of sensitivity indices calculated from Spearman and Pearson correlation coefficients (Input data: parameters included in "Group of nuclear data" and "Group of noise data", Output data: real and imaginary part of the absolute noise and the QoI).

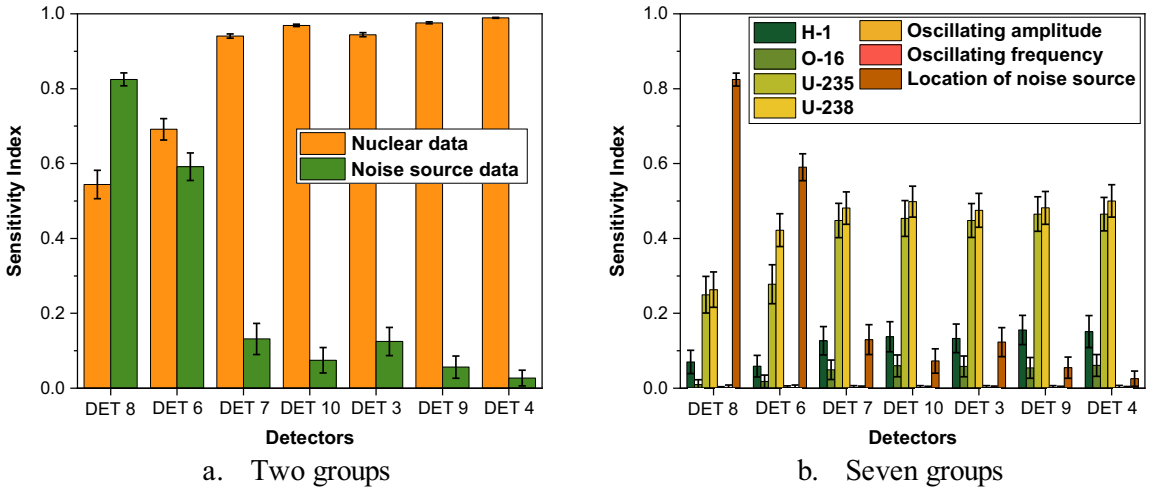

Fig. 13. The sensitivity indices and the 95% confidence intervals between grouped parameters (nuclear data group (one unified group and four isotope groups) and noise source data group (one unified group and three independent parameters)) and the QoI at different detector locations.

three parameters are included in "Group of noise source data", the covariance matrix to estimate in Equation (8) is small and its components converge quickly. However, "Group of nuclear data" consists of 748 correlated parameters, thus, an accurate estimation of its component will require a much larger number of samples; this explains the slow convergence of the associated sensitivity index. Therefore, it is expected that the sum of two groups sensitivity indices can become 1.0 eventually, when the sample size becomes large enough to result in a precise covariance matrix of "Group of nuclear data".

Nevertheless, when comparing the relative contributions of groups to the output uncertainty shown in Fig. 11, the "ranks between the two groups (groups of nuclear data and noise source data)" are identical to what can be seen in Fig. 13-a. Accordingly, it can be said that the qualitative ranks of the groups, which are obtained in this study with 1000 samples, are still reliable even though the quantitative estimates are not reliable.

Finally, the group of nuclear data is further divided by isotopes (U-235, U-238, H-1 and O-16). Additionally, the group of noise source data is divided into its individual parameters (oscillating amplitude, oscillating frequency, and location of noise source). At the location of Detectors 6 and 8, the QoI is strongly driven by the location of the noise source. At the remaining detector locations, the groups of U-235 and U-238 are the largest contributor to the QoI uncertainty.

Another finding is the irrelevance of the oscillating frequency for the amplitude of neutron noise. This can be explained by the Zero-Power reactor Transfer Function (ZPTF). Since CROCUS is a small-sized zero-power reactor, the dynamic behavior of the reactor is overwhelmingly driven by point-kinetics. In this condition, the reactor response is given by the ZPTF, whose "plateau region" exists in the specific frequency range of (Cacuci, 2010);

$$\lambda \ll \omega \ll \frac{\beta}{\Lambda_0}. \tag{10}$$

In this "plateau region", the oscillating frequency has very little impact on the reactor response and the amplitude of the neutron noise is nearly constant. Approximately, this range corresponds to the oscillating frequency between 0.01Hz and 20Hz, considering the characteristics of the CROCUS reactor (Kasemeyer, 2007). That is to say, the oscillating frequency in this study, 1Hz, belongs to the plateau region and this backs up the little effect on the QoI.

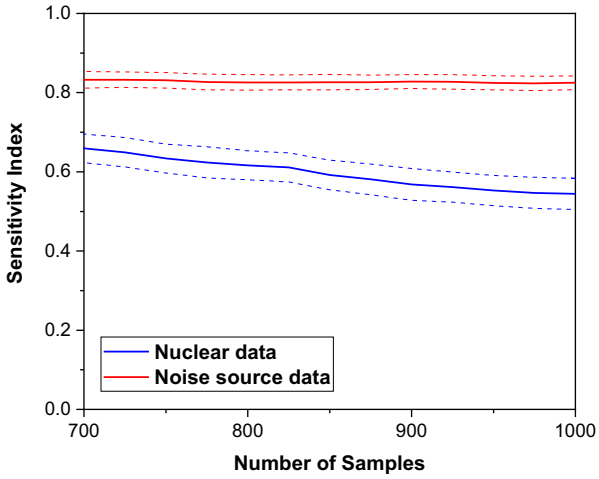

Fig. 14. The sensitivity indices of two groups with 95% confidence intervals varying with sample size (The straight line and the dashed line signify "mean value" and "95% confidence intervals", respectively.).

6. Conclusions

In this paper we have developed a methodology for uncertainty and sensitivity analysis for the simulation tools modeling the neutron noise distribution in critical reactors and applied it to an experiment carried out at a zero-power reactor. The noise source corresponds to the vibration of a group of fuel rods.

Based on the stochastic sampling-based method, the selected input parameters were perturbed according to their uncertainty distributions 300 times. The 300 input sets were served as inputs for the noise simulation using CORE SIM + to generate 300 QoIs at various detector locations.

The obtained outputs were used to determine the uncertainties and correlations among the QoIs. These correlations allow classifying the detectors into two groups, the detectors near the noise source and further away from the noise source. The uncertainties of the QoIs were determined by using the 4th order Wilks' formula for two-sided limits. The normality tests showed that the uncertainty of the absolute neutron noise is normally distributed, while the uncertainty of the QoI is not.

The sensitivity analyses were carried out using two different approaches. In the first approach, the input parameters were

separated into three independent groups. The three groups corresponded to "group of design and operating parameters", "group of nuclear data" and "group of noise source data". This approach ranked the groups of parameters by comparing the uncertainties of the QoIs, which were obtained by the perturbation of the input parameters included in each group. The results showed that the "group of design and operating parameters" had a negligible effect on the QoI and the two remaining groups mainly influenced the QoI.

The second approach involved a calculation of multiple correlation coefficients within grouped parameters to measure the sensitivity index of each group. Here the sample size was increased to 1000. The group of design and operating parameters was excluded from the study. The analysis which was performed with seven new groups (four groups of isotopes and three groups of noise source parameters) confirmed that the "location of noise source" and the two groups with "U-235" and "U-238" affect the QoI dominantly at the location near the noise source and the remaining area further away from the source, respectively.

Even though this work was carried out based on the specific condition and characteristics of a zero-power reactor, the established methodology could be replicated for the analysis of neutron noise in nuclear power plants.

CRediT authorship contribution statement

S. Yum: Conceptualization, Methodology, Formal analysis, Visualization, Writing – original draft, Writing – review & editing. **M. Hursin:** Conceptualization, Supervision, Methodology, Writing – original draft, Writing – review & editing. **A. Vasiliev:** Conceptualization, Writing – review & editing. **P. Vinai:** Conceptualization, Methodology, Writing – review & editing. **A.G. Mylonakis:** Conceptualization, Supervision, Methodology, Software, Writing – review & editing. **C. Demazière:** Conceptualization, Supervision, Methodology, Writing – review & editing. **R. Macián-Juan:** Conceptualization, Supervision, Writing – review & editing.

Declaration of Competing Interest

The authors declare that they have no known competing financial interests or personal relationships that could have appeared to influence the work reported in this paper.

Acknowledgements

The CORTEX research project has received funding from the Euratom research and training programme 2014-2018 under grant agreement No 754316. Additionally, this work was supported by a grant from the Swiss National Supercomputing Centre (CSCS) under project ID sm34.

References

Bundesamt für Strahlenschutz, 2012. Kurzbeschreibung und Bewertung der meldpflichtigen Ereignisse in Kernkraftwerken und Forschungsreaktoren der Bundesrepublik Deutschland im Zeitraum Januar 2011. Stand 14.12.2012.

Almaraz Trillo Report, 2012. Neutron noise status in Trillo NPP. Technical report CO-12/043, Spain.

Zwermann, W., Aures, A., Gallner, L., Hannstein, V., Krzykacz-hausmann, B., Velkov, K., Martinez, J.S., 2014. Nuclear data uncertainty and sensitivity analysis with XSUSA for fuel assembly depletion calculations. Nuclear Engineering and Technology 46 (3), 343–352.

Buss, O., Hoefer, A., Neuber, J.C., 2011. NUDUNA-Nuclear Data Uncertainty Analysis. In Proceedings of the International Conference on Nuclear Criticality (ICNC2011).

Bostelmann, F. et al., 2015. Sampling-based Nuclear Data Uncertainty Analysis in Criticality and Depletion Calculations. In Proceedings of the ANS MC2015.

Rochman, D. et al., 2016. Nuclear data uncertainty for criticality-safety: Monte Carlo vs. linear perturbation. Annals of Nuclear Energy 92, 150–160.

CORTEX project, 2017 http://cortex-h2020.eu/about-cortex.

M. Hursin, et al., 2018. Determination of Sobol Sensitivity Indices for Correlated Inputs with SHARK-X. PHYSOR 2018, Cancun, Mexico, April 22-26.

Iwamoto, H., Stakovskiy, A., Fiorito, L., Van den Eynde, G., de Saint Jean, C., 2018. Sensitivity and uncertainty analysis of βeff for MYRRHA using a Monte Carlo technique. EPJ Nuclear Sciences & Technologies 4, 42.

Rochman, D. et al., 2011. Nuclear data uncertainty propagation: Perturbation vs. Monte Carlo. Annals of Nuclear Energy 38, 942–952.

F. Bostelmann, et al., 2015. Uncertainty and Sensitivity Analysis in Criticality Calculations with Perturbation Theory and Sampling. M&C+SNA+MC 2015, Nashville, TN, USA, April 19-23.

L. Fiorito, 2016. Nuclear Data Uncertainty Propagation and Uncertainty Quantification in Nuclear Codes. Ph.D. Thesis, Universite Libre de Bruxelles, Bruxelles, Belgium, October 3.

B.T. Rearden, 2015. Criticality safety enhancements for scale 6.2 and beyond. In Proceedings of the International Conference Nuclear Criticality Safety (ICNC2015), Charlotte, NC, USA, September 13–17.

Rochman, D., Dokhane, A., Vasiliev, A., Ferroukhi, H., Hursin, M., 2020. Nuclear data uncertainties for core parameters based on Swiss BWR operated cycles. Annals of Nuclear Energy 148, 107727.

Yi, H., 2017. Uncertainty and Sensitivity Analysis for Nuclear Reactor Noise Simulations. In: Master's Degree thesis, Department of Physics. Chalmers University of Technology, CTH-NT-330.

H. Yi, P. Vinai, and C. Demazière, 2018. A sensitivity study for reactor neutron noise calculations with a neutron absorber of variable strength. PHYSOR 2018, Cancun, Mexico, April 22–26.

V. Lamirand, M. Hursin, P. Frajtag, and A. Pautz, 2016. Future Experimental Programmes in the CROCUS Reactor. RRFM/IGORR 2016, Berlin, Germany, March 13–17.

Lamirand, V. et al., 2018. Experimental report of the 1st campaign at AKR-2 and CROCUS. Technical Report D2.1 http://cortex-h2020.eu/wp-content/uploads/2019/07/CORTEX_D2_1_Experimental_Report_of_the_1st_Campaign_at_AKR2_and_CROCUS_V1.pdf.

Mylonakis, A. et al., 2021. CORE SIM+: A flexible diffusion-based solver for neutron noise simulations. Annals of Nuclear Energy 155, 108149.

U.S. NRC, 1999. Setpoint for Safety-Related Instrumentation. U.S. NRC Regulatory Guide 1 (105), Rev.3.

Vinai, P. et al., 2021. Final validation report. Technical Report D2.5 https://cortex-h2020.eu/wp-content/uploads/2021/09/CORTEX_D2_5_Final_validation_report_V1.pdf.

Demazière, C., 2011. CORE SIM: A multi-purpose neutronic tool for research and education. Annals of Nuclear Energy 38, 2698–2718.

Demazière, C. et al., 2019. Description of scenarios for the simulated data. Technical Report D3.1 http://cortex-h2020.eu/wp-content/uploads/2019/07/CORTEX_D3_1_Description_of_scenarios_for_the_simulated_data_V1.pdf.

Jonsson, A., Tran, H.N., Dykin, V., Pázsit, I., 2012. Analytical investigation of the properties of neutron noise induced by vibrating absorber and control rods. Kerntechnik 77 (5), 371–380.

Rais, A. et al., 2017. Neutronics modelling of the CROCUS reactor with SERPENT and PARCS codes. M&C 2017-International Conference on Mathematics & Computational Methods Applied to Nuclear Science & Engineering.

A. Rais, 2018. PARCS code model of the CROCUS reactor. CORTEX project internal technical report.

Leppänen, J., Aufiero, M., Fridman, E., Rachamin, R., van der Marck, S., 2014. Calculation of effective point kinetics parameters in the Serpent 2 Monte Carlo code. Annals of Nuclear Energy 65, 272–279.

Newland, D.E., 2012. An Introduction to Random Vibrations, Spectral and Wavelet Analysis. Dover Publications, Incorporated.

M. Hursin, 2021. Meeting minutes. Video conference for CORTEX work package 1 and 2, June 4, 2021, CORTEX consortium.

Zhu, T., 2015. Sampling-Based Nuclear Data Uncertainty Quantification for Continuous Energy Monte Carlo Codes. École Polytechnique Fédérale de Lausanne, Lausanne, Switzerland. PhD thesis.

Zhu, T., Vasiliev, A., Ferroukhi, H., Pautz, A., Tarantola, S., 2015. NUSS-RF: stochastic sampling-based tool for nuclear data sensitivity and uncertainty quantification. Journal of Nuclear Science and technology 52 (7–8), 1000–1007.

Cacuci, D.G. (Ed.), 2010. Handbook of Nuclear Engineering. Springer US, Boston, MA.

Zhu, T., Vasiliev, A., Ferroukhi, H., Pautz, A., 2015. NUSS: A tool for propagating multigroup nuclear data covariances in pointwise ACE-formatted nuclear data using stochastic sampling method. Annals of Nuclear Energy 75, 713–722.

M. Hursin, 2020. PMAX_samples_update_June2020.tar. Chalmers University FTP (core54.nephy.chalmers.se) /export/zh4/cortex/epfl/PERTURBEDXS/, Unpublished raw data.

Kasemeyer, U. et al., 2007. Physics of Plutonium Recycling, volume IX, Benchmark on Kinetic Parameters in the CROCUS Reactor. Reports to OECD/NEA Nuclear Science Committee (ISBN 978-92-64-99020-3).

Kloos, M., Hofer, E., 1999. SUSA - PC, a personal computer version of the program system for uncertainty and sensitivity analysis of results from computer models, version 3.2. user's guide and tutorial. Gesellschaft für Anlagen- und Reaktorsicherheit, Garching, Germany.

F. Reventós, 2008. Major Results of the OECD BEMUSE (Best Estimate Methods, Uncertainty and Sensitivity Evaluation) Programme. THICKET-2008, Pisa, Italy, May 5–9.

N. W. Porter, 2019. Wilks' Formula Applied to Computational Tools: A Practical Discussion and Verification. Sandia National Laboratories Report (SAND2019-1901J).
Yum, S. et al., 2019. Methodology for uncertainty and sensitivity analysis. Technical Report D1.1 http://cortex-h2020.eu/wp-content/uploads/2019/07/CORTEX_D1_1_Methodology_for_uncertainty_and_sensitivity_analysis_V1.pdf.
Demazière, C., 2011. Description of the models and algorithms used in the CORE SIM neutronic tool. Chalmers University of Technology, CTH-NT-241.
Conover, W.J., 1980. Practical Nonparametric Statistics. John wiley & Sons, New York.
Ramsey, P.H., 1989. Critical Values for Spearman's Rank Order Correlation. Journal of Educational Statistics 14 (3), 245–253.
S. Kajuri, 2018. Application of Hypothesis Testing and Spearman's rank correlation coefficient to demystify Suicides worldwide. https://towardsdatascience.com/application-of-hypothesis-testing-and-spearmans-rank-correlation-coefficient-to-demystify-b3a554730c91.
Bluman, A.G., 2009. Elementary Statistics: A Brief Version. McGraw-Hill, New York.
Shapiro, S.S., Wilk, M.B., 1965. An Analysis of Variance Test for Normality (Complete Samples). Biometrika 52 (3/4), 591–611.
Hsieh, N.-H., Reisfeld, B., Bois, F.Y., Chiu, W.A., 2018. Applying a Global Sensitivity Analysis Workflow to Improve the Computational Efficiencies in Physiologically-Based Pharmacokinetic Modeling. Front. Pharmacol. 9. https://doi.org/10.3389/fphar.2018.00588.
Sarrazin, F., Pianosi, F., Wagener, T., 2016. Global Sensitivity Analysis of environmental models: Convergence and Validation. Environmental Modelling & Software 79, 135–152.
V. Lamirand et al., 2020. Analysis of the First COLIBRI Fuel Rods Oscillation Campaign in the CROCUS Reactor for the European Project CORTEX. PHYSOR 2020, Cambridge, United Kingdom, March 29–April 2.
Kent State University, 2021. SPSS Tutorials: Pearson Correlation. https://libquides.library.kent.edu/SPSS.